

Short range Tb³⁺ spin correlations far above the two dimensional Néel temperature in Pb₂Sr₂TbCu₃O₈

U. Staub, L. Soderholm, and S. Skanthakumar

RECEIVED

MAR 13 1996

Argonne National Laboratory, Argonne, IL-60439-4814 OSTI

Abstract:

Whereas the Tb³⁺ moments undergo antiferromagnetic ordering at $T_N=5.5K$, our susceptibility and inelastic neutron scattering experiments indicate that significant magnetic Tb - Tb short range correlations persist to temperatures $T \geq 100K$. Magnetic correlations at such high temperatures relative to T_N are very unusual and they may shed new light on the relation between superconductivity and rare earth magnetism in these systems.

PACs: 71.70.ch Crystal field
 75.40.-s Short-range order
 74.72.-h High T_c superconductivity
 71.70.Gm Exchange interaction

The submitted manuscript has been authored by a contractor of the U. S. Government under contract No. W-31-109-ENG-38. Accordingly, the U. S. Government retains a nonexclusive, royalty-free license to publish or reproduce the published form of this contribution, or allow others to do so, for U. S. Government purposes.

MASTER

DISTRIBUTION OF THIS DOCUMENT IS UNLIMITED
 DISTRIBUTION OF THIS DOCUMENT IS UNLIMITED *ok*

The magnetic properties of rare earth doped high temperature superconductors are very interesting, exhibiting a variety of unusual magnetic ordering phenomena. The rare-earth sublattice shows 3 dimensional (3D) long range, [1,2] 3D with finite correlation length [3], 2D, [4,5] and hyperfine-field induced magnetic ordering [3]. In addition, some of these compounds, including their parent compounds, exhibits 2D short range correlations well above the Néel temperature [1]. One interesting system is $\text{Pb}_2\text{Sr}_2\text{TbCu}_3\text{O}_8$, which exhibits a 2D long range ordering temperature at $T_N=5.5\text{K}$, and 2D short range correlations reported up to 10K. [6]

$\text{Pb}_2\text{Sr}_2\text{RCu}_3\text{O}_8$ (R=rare earth) are layered materials which are structurally complex, but basically similar to the other copper oxide systems such as the $\text{RBa}_2\text{Cu}_3\text{O}_x$ series or the Tl- and Bi-based cuprates. The isostructural R=Tb analog of $\text{Pb}_2\text{Sr}_2\text{RCu}_3\text{O}_8$ does form and by replacing 50% of Tb with Ca, it becomes a superconductor with $T_c = 84\text{K}$. Work on a related system $\text{Tb}_{0.1}\text{Y}_{0.9}\text{Ba}_2\text{Cu}_3\text{O}_x$ has shown that the Tb ion retains a localized trivalent character [7]. For a better understanding of the magnetic properties, information on the magnetic rare earth ionic ground-state wave functions and the exchange interaction is required. This can be obtained by measuring the crystalline electric-field (CEF) excitations using inelastic neutron scattering (INS).

In this work, we report INS and magnetic susceptibility data that should help to develop a better understanding of magnetic short range correlations well above T_N . Below $\sim 120\text{K}$ the observed susceptibilities obtained from single-crystal measurements deviate from the calculated susceptibilities. The INS experiments indicate an onset temperature for short range spin correlations at $T \geq 100\text{K}$, which is more than an order of magnitude higher than the 2D ordering temperature (5.5K) found previously by neutron diffraction [6].

Details about the sample preparation and characterization are given elsewhere [8]. Inelastic neutron scattering experiments were carried out on the High-Resolution Medium-Energy Chopper Spectrometer (HREMCS) at the Intense Pulsed Neutron Source (IPNS) of Argonne National Laboratory. Using an incident neutron energy (E_i) of 4 meV the energy resolution (full width at half maximum) is ~ 0.175 meV in the elastic region. A 50 g powder sample was enclosed in a flat aluminum container of 8 cm high and 6 cm wide and then attached to the cold finger of a closed-cycle helium refrigerator for measurements between 20 to 200K. A conventional helium cryostat was used for the low temperature ($1.5 \text{ K} \leq T \leq 20 \text{ K}$) experiments. The raw data were corrected for detector efficiency and background scattering by standard procedures. Neutron absorption by the sample was found to be negligible.

The magnetic susceptibility experiments were performed on a SQUID magnetometer over the temperature range of 10 to 300K using an applied field of 500 Oe. A ~ 1 mg single crystal was attached directly to a quartz fiber. Measurements were made with the "long" crystallographic c axis perpendicular and parallel to the applied field. Pellets of about 100 mg were used for the measurements on the polycrystalline samples.

For crystal-field calculations we use a Hamiltonian which includes the free ion interactions, as described elsewhere [9]. The Tb^{+3} free-ion parameters are taken from those of Tb in LaF_3 [10]. The experimentally observed CEF transitions and the description of the CEF potential are the subject of another publication [8]. In this work we use the CEF parameters obtained from an extrapolation from those of $\text{Pb}_2\text{Sr}_2\text{HoCu}_3\text{O}_8$ [11]. It was shown previously that such an extrapolation of the CEF parameters between different rare earths in the same crystal host give an accurate description of the CEF splitting [12]. Here we note that the calculated magnetic susceptibilities are only weakly

dependent on the exact CEF parameters chosen. One of the important features of the derived CEF level scheme is that the Γ_4 ground-state and the first excited state Γ_3 are separated in energy by only $7 \mu\text{eV}$. The transition strength between these two states is so strong that this transition accounts for about 90% of the intensity expected for the whole J-multiplet.

The susceptibilities of $\text{Pb}_2\text{Sr}_2\text{TbCu}_3\text{O}_8$ and a magnetically dilute $\text{Pb}_2\text{Sr}_2\text{Y}_{0.95}\text{Tb}_{0.05}\text{Cu}_3\text{O}_8$ are shown in Figure 1. For the magnetically dilute system, the susceptibility is well represented by the calculation whereas for the undilute system χ is considerably reduced compared to the calculation and to the dilute system at temperatures below about 120 K. Therefore, the starting point of this deviation is interpreted as the onset temperature for antiferromagnetic Tb - Tb spin correlations. Surprisingly, this temperature is more than an order of magnitude higher than the 2D ordering temperature of 5.5K. In the inset of figure 1 we compare the measured susceptibilities of a single crystal of $\text{Pb}_2\text{Sr}_2\text{TbCu}_3\text{O}_8$ with the single-ion susceptibilities obtained from a CEF calculation. The susceptibilities exhibit strong anisotropy between the in plane χ^\perp and out of plane χ^\parallel components. The calculation shows that this anisotropy originates from the crystalline electric-field imposed by the ligands. However, the observed χ deviates considerably from the calculation at temperatures below about 120 K. This supports our view, that we can designate this starting point of deviation as the onset temperature for short-range spin correlations. The upturn in χ^\perp around 30 K can be understood in terms of an additional transverse component in the longitudinal transition between the two lowest CEF states.

We calculate the influence of the magnetic ordering on the CEF splitting between the Γ_4 and the Γ_3 state using a mean-field (MF) approximation. The mean-field parameter λ is defined as $\chi^{\text{zz}}(T_N)^{-1} = \lambda$, where T_N is the 2D Néel temperature of 5.5 K and χ_0 is the calculated single ion susceptibility.

Using this equation, we obtain a mean-field parameter of $5.0 \mu\text{eV}$. This value is slightly smaller than the corresponding one for Ho^{+3} in $\text{HoBa}_2\text{Cu}_3\text{O}_7$, which was derived from the zero-field magnetization [3]. The relatively high Néel temperature of 5.5K can be understood with the same strength of the exchange interaction (λ) as in the $\text{RBa}_2\text{Cu}_3\text{O}_7$ system, indicating that there is no significant hybridization between the Tb and the CuO_2 bands. Using the Hamiltonian $\mathbf{H}_{\text{FI}}+\mathbf{H}_{\text{CEF}}+\mathbf{H}_{\text{mf}}$, where $\mathbf{H}_{\text{FI}}+\mathbf{H}_{\text{CEF}}$ is the sum of free-ion and CEF Hamiltonians and $\mathbf{H}_{\text{mf}} = \lambda \langle J \rangle^z \mathbf{J}^z$, we arrived at an ordered moment for Tb^{+3} at 1.5 K of $\mu_{\text{sat}} = 8.67 \mu_{\text{B}}$. This ordered moment is higher than that ($7.43 \pm 0.02 \mu_{\text{B}}$) obtained by powder neutron diffraction [6]. The over estimation of the calculated moment could be explained by the fact that the MF approximation is inadequate in the region where spin fluctuations are strong. In addition, we know that this system favors a 2D Ising type of interaction. The calculated energy splitting of the quasi-doublet in the MF approximation is 0.5 meV at 1.5K , and the transition strength is too small to be seen experimentally (see Table I).

The INS spectra obtained at 1.5 K (well below T_{N}) and at 20K (well above T_{N}) are shown in Figure 2. There are no observable inelastic magnetic transitions at either temperature, nor is there any additional quasi-elastic contribution. The full width at half maximum of the elastic line is $0.175 \pm 0.005 \text{ meV}$ for both temperatures and is limited by the instrumental resolution. Even when the expected energy of the CEF transition is too low in energy to observe directly, the half width of the transition, which is broadened by relaxations, exchange, and hybridization effects, should give rise to an observable broadening of the elastic line. Such a broadening is not observed at these temperatures. The only difference between the two spectra is the large difference in the intensities of the elastic line. For higher temperatures we

observe an additionally quasi-elastic contribution (see Figure 3) that increases with increasing temperature. This additional intensity is of magnetic origin as shown by its decreasing intensity with increasing Q . The CEF calculations show that the quasi-elastic intensity cannot be explained by excited CEF transitions between higher lying states.

To examine the temperature dependence of the two different magnetic intensities, we fitted them with a Gaussian and a Lorentzian function convoluted with the Gaussian resolution function of the instrument. In this analysis, we include only the low angle detectors corresponding to momentum transfers of $0.07 < Q < 0.44 \text{ \AA}^{-1}$. This Q -range is much below the first magnetic 2D-like Bragg reflection at $Q=1.15 \text{ \AA}^{-1}$ ($1/2, 1/2$; $a \approx b \approx 3.85 \text{ \AA}$; following the notation used by Wu et al [6]). Below 20K only the Gaussian components survive. We found that the Gaussian component remains resolution limited over the whole temperature range of 1.5 to 200K. The integrated intensity of the elastic and quasi-elastic line as a function of temperature is shown in Figure 4.

At 1.5K, in the regime of the "long range" ordering, the integrated Gaussian intensity corresponds to solely nuclear incoherent scattering. For higher temperatures ($T \geq 5 \text{ K}$), an additional magnetic contribution is observed due to the spread out the magnetic intensity in reciprocal space by a correlation length of the 2D ordered moments. In the paramagnetic region at 200 K, the observed magnetic intensity arises solely from the CEF transition between the two lowest states. It is represented by the magnetic quasi-elastic contribution shown in Figure 4. Assuming no short range correlation at $T=200\text{K}$, the integrated resolution Gaussian intensity corresponds to the nuclear incoherent scattering alone. We have an intermediate case at 100 K. The extra intensity of the resolution limited elastic line at 100K must be of magnetic origin. This view

is supported by the fact that the quasi-elastic intensity at 100K is reduced from the 200 K level so that the overall sum of both intensities remains constant.

In order to understand the relative intensity between the elastic and quasi-elastic components, we calculated the transition intensities within the Γ_4 ground-state and between the Γ_4 and the Γ_3 states at selected values of $g_j\langle J \rangle$ within the framework of the MF approximation. The results are listed in Table I. Comparing the experiment with the calculated transition strengths, we can define three different regions. The observation for $T \leq 20\text{K}$ is well represented by the MF approximation, with a large value of $g_j\langle J \rangle$. At 100 K a short range ordered moment of $g_j\langle J \rangle = 0.1 \mu_B$ describes well the observed intensities and for 200 K the system is well represented by the pure paramagnetic state.

This system may exhibit short range Tb-Tb correlations up to such high temperatures for several reasons. The very strong magnetic anisotropy couples with the 2 dimensional crystalline structure. The 2D ordering at low temperatures can be understood by a relatively strong 2D exchange interaction coupled with a weak dipole interaction parallel to the c axis that partly overcomes the thermal motion of the spins at 5.5 K. The 3D magnetic structure with finite correlation length can be seen in the powder neutron diffraction pattern at $T=1.5\text{K}$, where broad, asymmetric magnetic reflections $(1/2, 1/2, 2)$ and $(1/2, 1/2, 3)$ are observed [6]. The weak dipole interaction along c favours ferromagnetic coupling in this direction. The two lowest CEF states have the correct symmetry to be correlated strongly by a relatively small Ising type of interaction. This, and the fact that $J_{\perp} \gg J_{\parallel}$ give rise to the unusual magnetic properties exhibited in this system. Additional experimental information about the exchange interaction in these materials could further the understanding of the unusually high onset temperature of the spin fluctuations. However, $\text{HoBa}_2\text{Cu}_3\text{O}_7$ is the only related system where the exchange parameters have

been determined [13]. It was found, that the Ising-like exchange ($\mathbf{H} = -1/2 \sum_{i>j} J_{ij}^z \mathbf{J}_i^z \mathbf{J}_j^z$) is relatively strong with $J_a^z = -6.9 \mu eV$, even though this system does not favor an Ising type of interaction because of the symmetry of the two lowest CEF states. This results further supports our argument that the Ising type of interaction is important in the system under investigation here. The increase of the Lorentzian half width observed between 100K and 200K reflect a relaxation mechanism that is not yet understood.

In conclusion, the observed susceptibilities indicate Tb^{+3} short range correlation up to 120 K. The INS experiments are described in the mean-field approximation. These experiments strongly suggest $Tb - Tb$ short range correlations above 100K, more than an order of magnitude higher than the 2D ordering at 5.5 K. The three reasons for the very unusual behaviour are the very strong anisotropy in the susceptibility governed by the crystalline environment, the 2 dimensional type of the crystal structure, and the Ising type of exchange interaction in this particular system.

The authors wish to thank U. Welp (ANL) for help with the SQUID measurements, J. Simon Xue for loan of the single crystal and C-K. Loong for helpful discussions. Financial support by DOE-Basic Energy Sciences - Chemical Sciences, under contract W-31-109-ENG-38 and the Swiss National Science Foundation is gratefully acknowledged.

DISCLAIMER

This report was prepared as an account of work sponsored by an agency of the United States Government. Neither the United States Government nor any agency thereof, nor any of their employees, makes any warranty, express or implied, or assumes any legal liability or responsibility for the accuracy, completeness, or usefulness of any information, apparatus, product, or process disclosed, or represents that its use would not infringe privately owned rights. Reference herein to any specific commercial product, process, or service by trade name, trademark, manufacturer, or otherwise does not necessarily constitute or imply its endorsement, recommendation, or favoring by the United States Government or any agency thereof. The views and opinions of authors expressed herein do not necessarily state or reflect those of the United States Government or any agency thereof.

References

- 1 J. W. Lynn, in edited by J. W. Lynn (Springer, Berlin, 1990), p. 268.
- 2 B. Roessli, P. Allenspach, P. Fischer, J. Mesot, U. Staub, H. Maletta, P. Brüesch, C. Ritter, and A. W. Hewat, *Physica C* **180 & 181**, 396 (1992).
- 3 B. Roessli, P. Fischer, U. Staub, M. Zolliker, and A. Furrer, *Eur. Phys. Lett.* **23**, 511 (1993).
- 4 J. W. Lynn, *J. Alloys Comp.* **181**, 419 (1992).
- 5 B. Roessli, P. Fischer, M. Zolliker, P. Allenspach, J. Mesot, U. Staub, A. Furrer, E. Kaldis, B. Bucher, J. Karpinski, E. Jilek, and H. Mutka, *Z. Phys. B* **91**, 149 (1993).
- 6 S. Y. Wu, W. T. Hsieh, W.-H. Li, K. C. Lee, J. W. Lynn, and H. D. Yang, *J. Appl. Phys.* **75**, (1994).
- 7 U. Staub, M. R. Antonio, L. Soderholm, M. Guillaume, W. Hengeler, and A. Furrer, *Phys. Rev. B* **50**, in press. (1. September 1994).
- 8 U. Staub, L. Soderholm, S. Skanthakumar, Mark. R. Antonio, J. Simon Xue, and C.-K. Loong, to be published (1994-95).
- 9 J. Mesot, P. Allenspach, U. Staub, A. Furrer, H. Mutka, R. Osborn, and A. Taylor, *Phys. Rev B* **47**, 6027 (1993).
- 10 W. T. Carnall, G. L. Goodman, K. Rajnak, and R. S. Rana, *J. Chem. Phys.* **90**, 3443 (1989).
- 11 L. Soderholm, C.-K. Loong, J. S. Xue, J.P. Hammonds, J.E. Greedan, and M. Maric, *J. Appl. Phys.* **73**, 6314 (1993).
- 12 G.L. Goodman, C.-K. Loong, and L. Soderholm, *J. Phys.: Condens. Matter* **3**, 49 (1991).

13 U. Staub, F. Fauth, M. Guillaume, J. Mesot, A. Furrer, P. Dosanjh, H. Zhou, and P. Vorderwisch, *J. Appl. Phys.* **75**, 6334 (1994).

Table I Calculated transition strengths in the MF approximation for selected values of moments $g_j \langle J \rangle$. ($M_0^2 = \langle \Gamma_4^1 | \mathbf{L} + 2\mathbf{S} | \Gamma_4^1 \rangle^2$ and $M_1^2 = \langle \Gamma_3^1 | \mathbf{L} + 2\mathbf{S} | \Gamma_4^1 \rangle^2$)

$g_j \langle J \rangle$ [μB]	M_0^2	M_1^2
0	0	81.1
0.05	17.0	64.2
0.1	41.8	39.4
0.3	73.5	7.7
0.5	78.3	6.0
1	80.5	1.5

Figure captions:

- Fig. 1 Observed and calculated (line) polycrystalline susceptibilities versus temperature of $\text{Pb}_2\text{Sr}_2\text{TbCu}_3\text{O}_8$ (open circles) and $\text{Pb}_2\text{Sr}_2\text{Y}_{0.95}\text{Tb}_{0.05}\text{Cu}_3\text{O}_8$ (full circles) normalized per mole Tb. Inset: Observed and calculated (line) single crystal susceptibilities of $\text{Pb}_2\text{Sr}_2\text{TbCu}_3\text{O}_8$ (open squares //c, full squares //a,b).
- Fig. 2 Temperature dependence of elastic line taken for $\text{Pb}_2\text{Sr}_2\text{TbCu}_3\text{O}_8$ with $E_i=4$ meV and $0.07 < Q < 0.44 \text{ \AA}^{-1}$. The line corresponds to the fitted Gaussian function
- Fig. 3 Detailed balance corrected temperature dependence of the energy spectra from $\text{Pb}_2\text{Sr}_2\text{TbCu}_3\text{O}_8$ focused on the quasi-elastic contribution ($E_i = 4$ meV and $0.07 < Q < 0.44 \text{ \AA}^{-1}$). The solid line corresponds to the total fit, the broken line to the Lorentzian and the dotted line to the Gaussian.
- Fig. 4 Temperature dependence of the integrated elastic (open circles) and quasi-elastic intensity (full circles) for $0.07 < Q < 0.44 \text{ \AA}^{-1}$ and $E_i = 4$ meV. The solid lines are guide to the eyes. The dashed line represents the elastic nuclear incoherent scattering background.

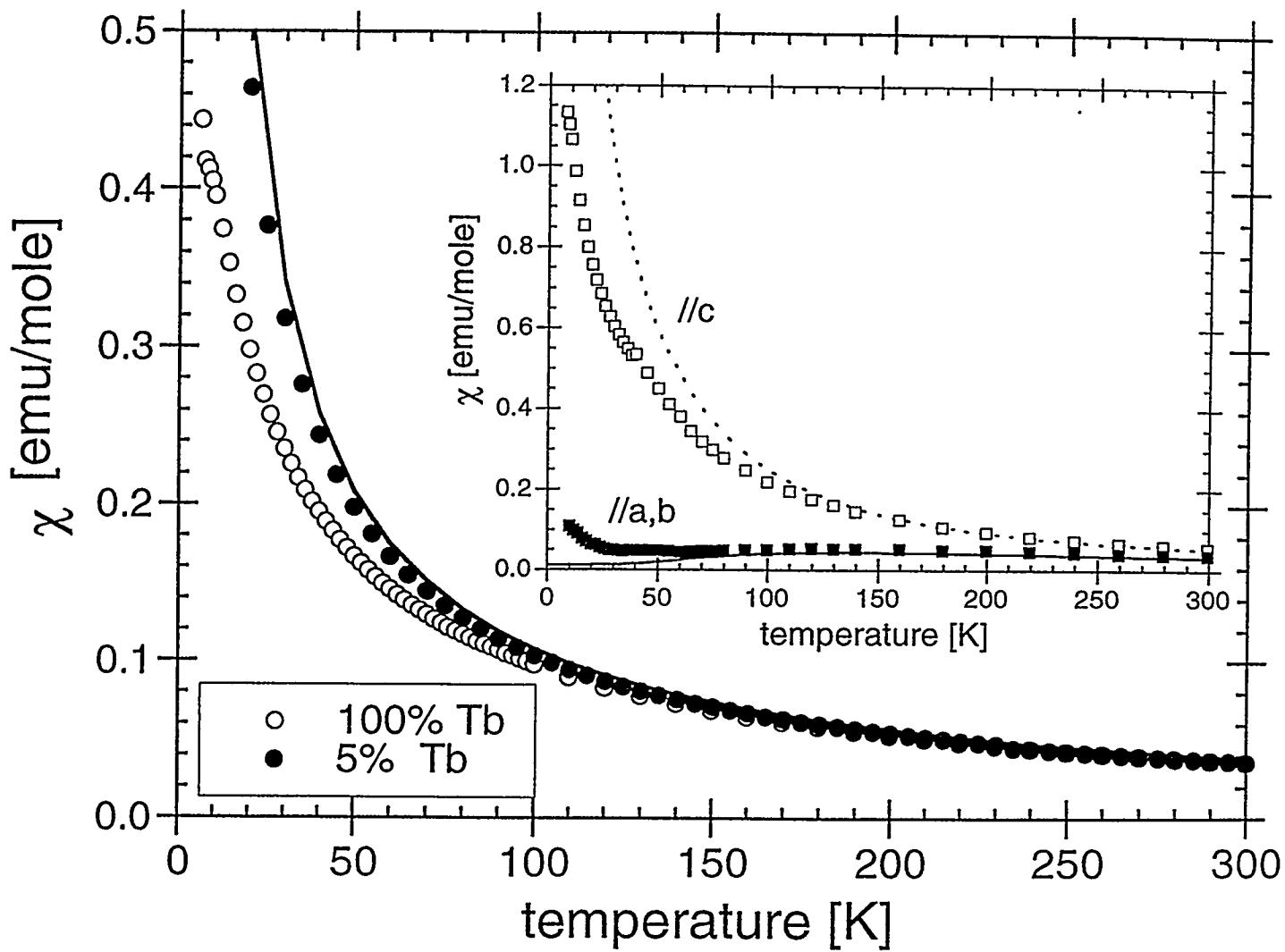


Fig. 1 χ [emu/mole]

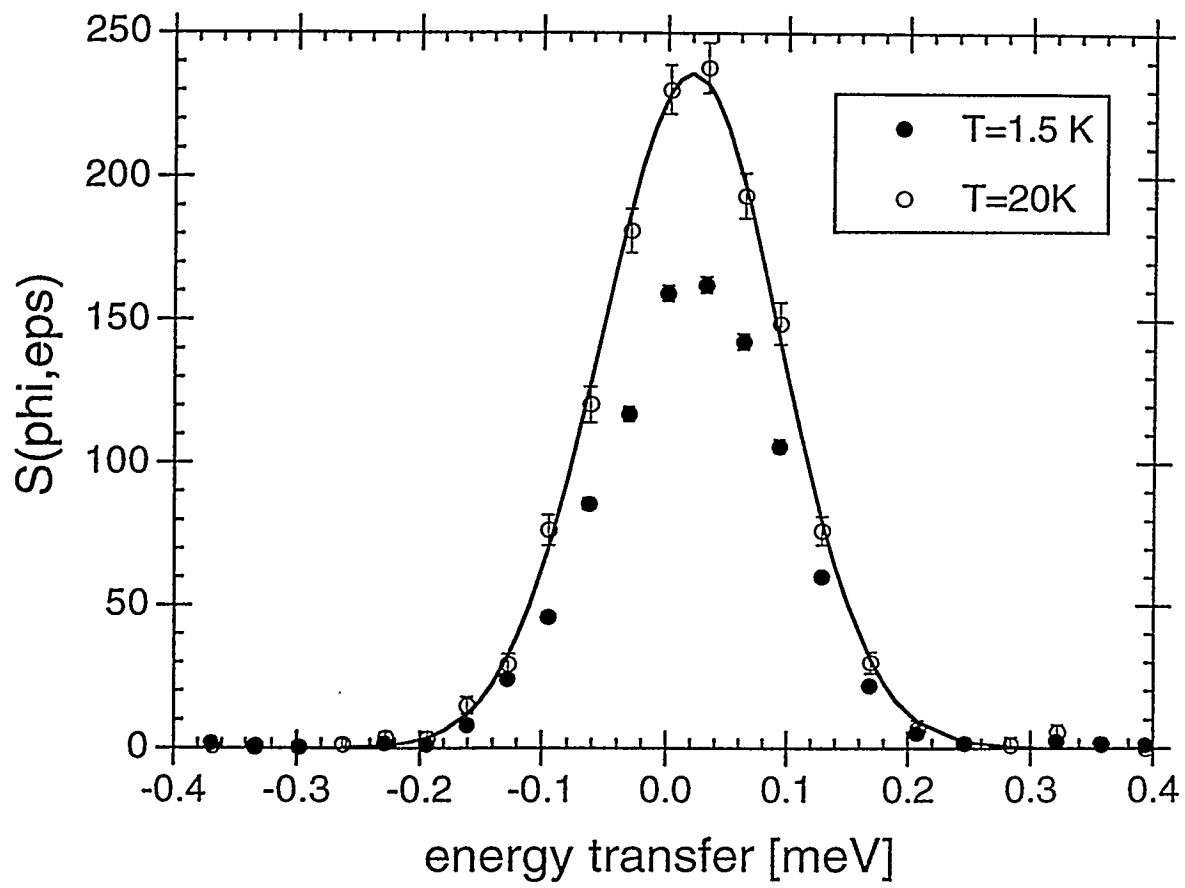


Fig. 2

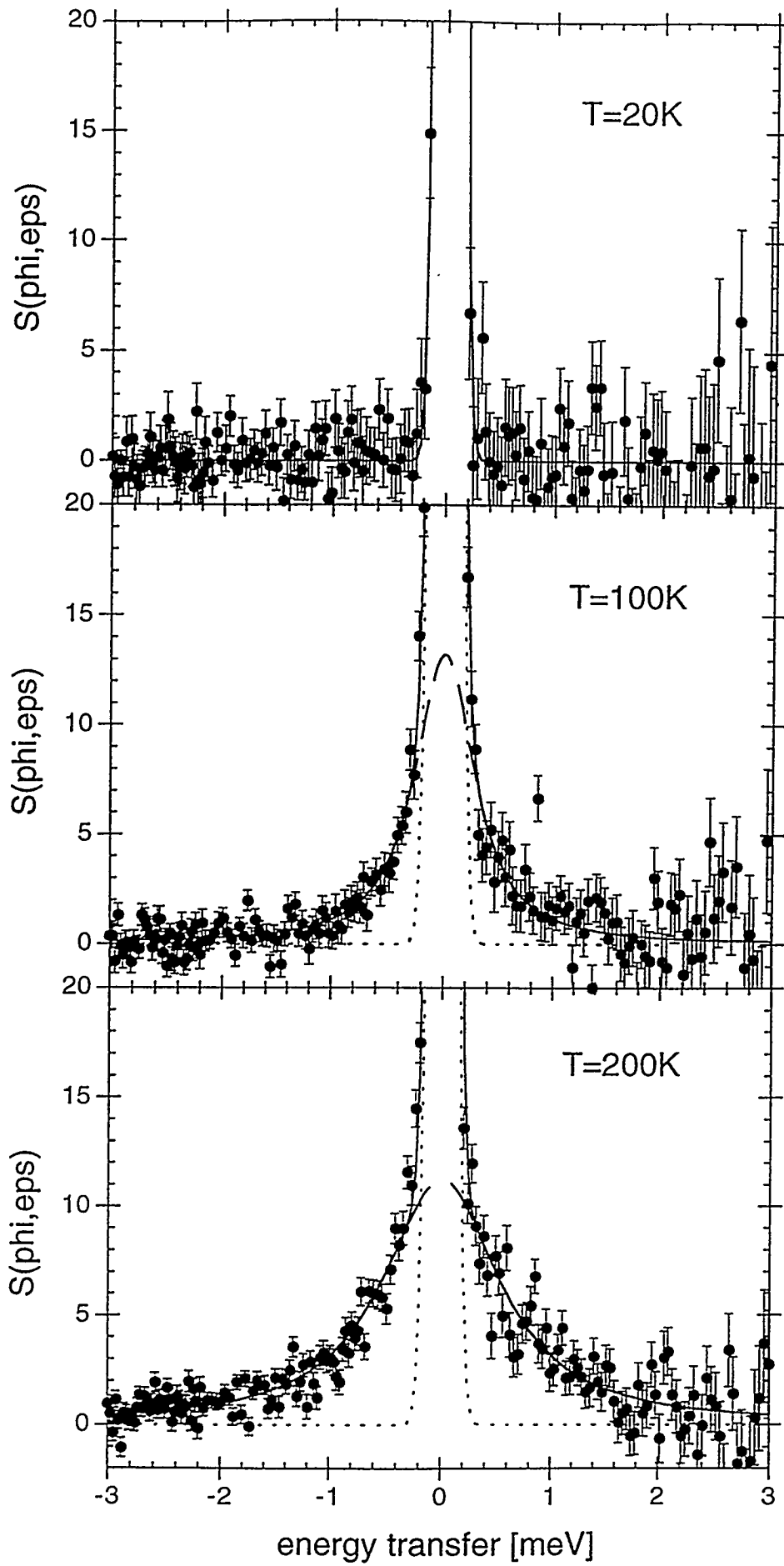


Fig. 3

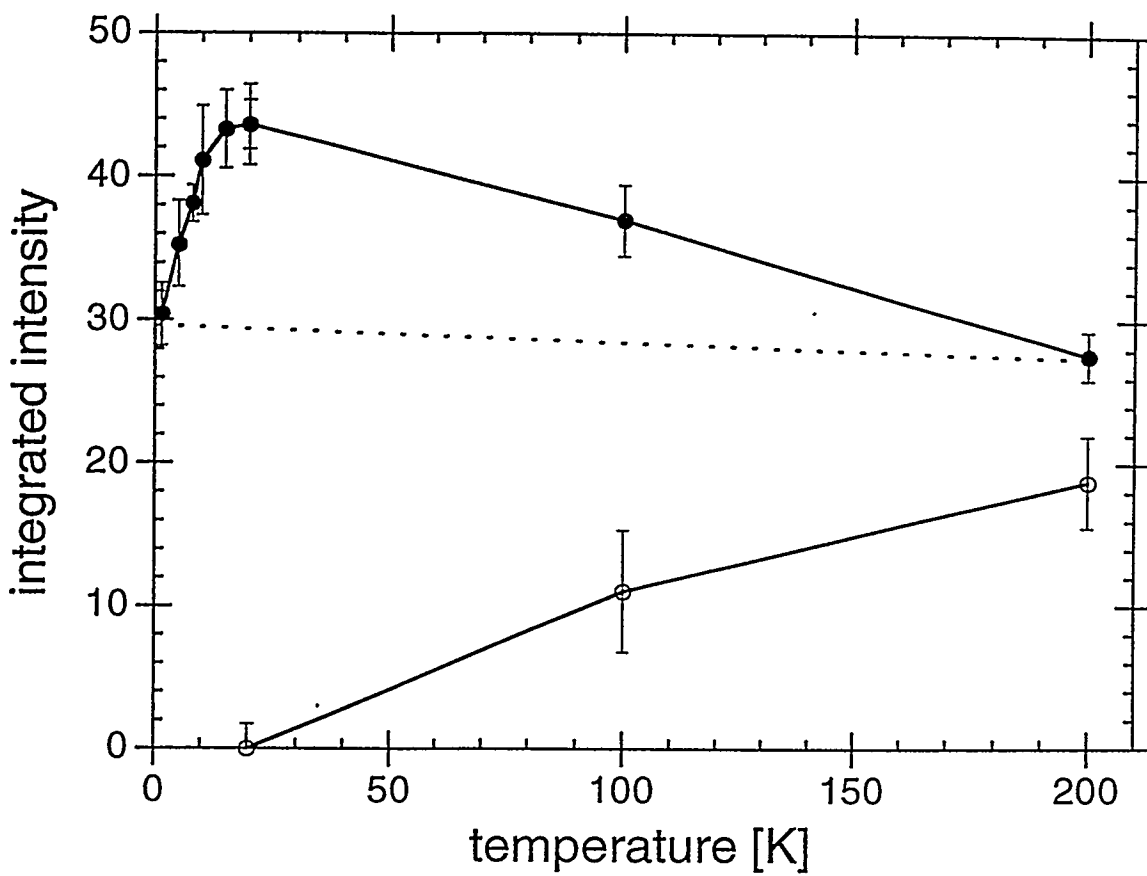


Fig. 4